



HAL
open science

Experiments and Numerical Modelling of Microbially-Catalysed Denitrification Reactions

Laurent André, H el ene Pauwels, Marie Christine Dictor, Marc Parmentier,
Mohamed Azaroual

► **To cite this version:**

Laurent Andr e, H el ene Pauwels, Marie Christine Dictor, Marc Parmentier, Mohamed Azaroual. Experiments and Numerical Modelling of Microbially-Catalysed Denitrification Reactions. *Chemical Geology*, 2011, 287, pp.171-181. 10.1016/j.chemgeo.2011.06.008 . hal-00617602

HAL Id: hal-00617602

<https://brgm.hal.science/hal-00617602>

Submitted on 29 Aug 2011

HAL is a multi-disciplinary open access archive for the deposit and dissemination of scientific research documents, whether they are published or not. The documents may come from teaching and research institutions in France or abroad, or from public or private research centers.

L'archive ouverte pluridisciplinaire **HAL**, est destin ee au d ep ot et  a la diffusion de documents scientifiques de niveau recherche, publi es ou non,  emanant des  tablissements d'enseignement et de recherche fran ais ou  trangers, des laboratoires publics ou priv es.

1
2
3
4
5
6
7
8
9
10
11
12
13
14
15
16
17
18
19
20
21
22
23
24
25
26
27
28
29
30
31
32

**Experiments and Numerical Modelling of Microbially-Catalysed
Denitrification Reactions**

By L. André*, H. Pauwels, M.-C. Dictor, M. Parmentier, M. Azaroual,

BRGM, 3 Avenue C. Guillemin, BP 36009, F-45060 Orléans Cedex 2, France

*** Corresponding author:**

Laurent ANDRE

l.andre@brgm.fr

Tel : +33 238 64 31 68

Fax : +33 238 64 37 19

Submitted to Chemical Geology

First submission December 2010

Revised manuscript April 2011

33 **Abstract**

34 Denitrification processes have been studied for many decades in both the laboratory and the
35 field, and current work investigates heterotrophic and autotrophic denitrification reactions.
36 Physical, chemical and microbiological parameters have been shown to control these
37 degradation processes and the fate of nitrogen. In this paper, we describe results and
38 modelling of denitrification reactions in batch and flow-through column experiments. The
39 processes controlling the fate of nitrate and, more specifically, its reduction mediated by
40 micro-organisms are explained in detail by a multi-step process. Modelling involves a rate
41 law describing microbial respiration. Batch experiment data and the results of thermo-kinetic
42 modelling of biogeochemical processes are in relatively good agreement, indicating that the
43 coupled numerical approach is suitable for simulating each individual mechanism involved in
44 denitrification phenomena. The calculated mass-balance indicates that about 40 % of the
45 carbon from acetate is used for anabolism and 60 % for catabolism. The kinetic parameters
46 estimated from the batch experiments are also suitable for reactive transport modelling of
47 laboratory flow-through column experiments. In these experiments performed on pyrite-
48 bearing schist, 80 % of the nitrate reduction is attributed to heterotrophic micro-organisms
49 and 20 % to autotrophic bacteria. These results also indicate that for denitrification in the
50 presence of acetate, the thermodynamic factor in the coupled thermodynamic/kinetic law can
51 be disregarded and denitrification kinetics will be governed, for the most part, by electron
52 donor/acceptor concentrations. This consistency between the results of closed and open
53 systems is a prerequisite for the field-scale use of this type of numerical approach and the
54 efficient and safe management of nitrogen sources. Breaking down the process into several
55 steps makes it possible to focus on the main parameters that enhance the denitrification rate.

56

57 **Keywords:** denitrification; thermodynamic driving force; kinetics; micro-organisms

58

59 **1. Introduction**

60 Groundwater nitrate (NO_3^-) concentrations exceed human health criteria in many places as a
61 result of anthropogenic inputs such as industrial emissions and synthetic fertilizers and
62 manure used in agriculture (Squillace et al., 2002; McCallum et al., 2008; and references
63 therein). Nitrate is now very commonly found in groundwater in Europe and North America
64 (Matějů et al, 1992; Rivett et al, 2008). This creates environmental problems and has even led
65 to the halting of pumping in many well fields. Techniques to decrease nitrate concentrations
66 include ion exchange, reverse osmosis and biological denitrification (Matějů et al, 1992).

67 Denitrification (or dissimilatory nitrate reduction) is recognised as being an efficient natural
68 microbially-mediated nitrogen removal process in soils and waters (Dahab, 1987; Rivett et al.,
69 2008; Aelion and Warttinger, 2010). Indeed, groundwater nitrate can be attenuated by
70 denitrification processes that reduce NO_3^- according to a series of reactions mediated by
71 micro-organisms under anaerobic conditions (Knowles, 1982; Tavares et al., 2006; Rivett et
72 al., 2008):



74 This has been widely observed in natural environments such as wetlands (Bowden, 1987;
75 Whitmire and Hamilton, 2005; Scott et al., 2008), hyporheic zones (Duff and Triska, 1990;
76 Jones et al., 1995; Sheibley et al., 2003) and shallow and deep aquifers (Lovley and Chapelle,
77 1995; Pauwels et al., 1998, 2010; Pinay and Burt, 2001; Molénat et al., 2002; Ruiz et al.,
78 2002). Denitrification, with either heterotrophic (Her and Huang, 1995; Aslan, 2005) or
79 autotrophic bacteria (Koenig and Liu, 2001; Park and Yoo, 2009), is also used to treat
80 drinking water.

81
82 All of these nitrate bioremediation processes use denitrifying bacteria, which, like other
83 micro-organisms in soil, water, sediments and oceans, play a major role in the biogeochemical
84 cycles of major and trace elements (carbon, nitrogen, sulphur, phosphorus, iron, mercury,
85 selenium, arsenic, etc.) (Dommergues and Manganot, 1970; Stevenson and Cole, 1999;
86 Madigan et al., 2000; Ehrlich, 2002). Most of these bacteria are able to use the energy of
87 redox reactions to proliferate under aerobic or anaerobic conditions (Decker et al., 1970;
88 Mitchell, 1961). They act as a catalyst for reactions in which electrons are transferred from a
89 donor to an acceptor species. This microbial activity also links electron transfer to proton
90 transfer through the cell membrane, enabling the synthesis of adenosine triphosphate (ATP)
91 from adenosine diphosphate (ADP) and intracellular phosphate ions (P_i). However, this
92 reaction occurs only if the energy of the corresponding redox reaction is high enough to
93 provide the energy for bacterial metabolism as an excess enthalpy (Jin and Bethke, 2002).
94 Bacterial behaviour in natural aqueous systems is therefore closely linked to redox reactions
95 (Lindberg and Runnels, 1984; Keating and Bahr, 1998; Michard, 2002).

96
97 These observations highlight the connexions between chemical and biological processes and
98 the need to take into account a coupled thermodynamic/kinetic approach in order to accurately
99 predict the global behaviour of such systems. Many theoretical and empirical approaches have

100 been developed to describe biogeochemical processes. These include the enzyme reaction
101 kinetic model proposed by Michaelis and Menten (1913) and the bacterial growth kinetics
102 model proposed by Monod (1949). The latter is used most often to describe the relationship
103 between bacterial growth and substrate concentration (Rittmann and McCarty, 2001). This
104 approach, while very successful for batch systems, has significant limitations. It is suitable for
105 irreversible reactions and conditions far from thermodynamic equilibrium where chemical
106 energy is not a limiting factor (Curtis, 2003; Jin and Bethke, 2007; Torres et al., 2010). It
107 cannot, however, correctly predict reaction rates when substrate concentrations drop below a
108 substrate threshold value (Lovley, 1985, Cord-Ruwisch et al., 1988; Giraldo-Gomez et al.,
109 1992). Like other empirical rate laws, it does not consider that, close to thermodynamic
110 equilibrium, there is not enough available energy to meet the needs of micro-organisms for
111 microbial metabolism, maintenance and other cellular functions (Jin and Bethke, 2007).

112

113 Because of the large number and the complexity of the elementary mechanisms involved, the
114 numerical modelling of these processes requires the use of powerful and relevant theoretical
115 approaches in the calculation codes. To enable us to progress in our understanding of the
116 biogeochemical behaviour of ecosystems, robust numerical tools must consider not only
117 chemical and thermodynamic processes (i.e. Gibbs free enthalpy of the redox reactions), but
118 also biological phenomena (i.e. bacterial growth). Among the various patterns proposed to
119 simulate these coupled processes, that of Jin and Bethke (2003, 2005, 2007) appears to be the
120 most comprehensive because it considers both the chemical characteristics of the system
121 (through electron donor/acceptor concentrations) and thermodynamic conditions (through the
122 Gibbs free enthalpy of the redox reactions involved), which are the driving forces of the
123 biogeochemical processes. The suitability of this approach (thereafter called "the Jin and
124 Bethke approach") and the role of the thermodynamic potential factor have been
125 demonstrated for degradation processes with the thermodynamic control of the respiration
126 rate during arsenate reduction (Jin and Bethke, 2003), methanogenesis or sulfate reduction
127 (Jin and Bethke, 2005). In these examples, the respiration process is expected to cease, even if
128 significant amounts of both electron donors and acceptors are still available for
129 metabolization. The role of thermodynamics has also been described concerning the progress
130 of enzymatic reactions like benzoate, crotonate and glucose fermentations (Jin and Bethke,
131 2007).

132

133 Because denitrification is a complex process mediated by micro-organisms, this coupled
134 thermokinetic/biogeochemical approach would seem to be highly suitable for simulating the
135 biogeochemical reactions occurring between nitrate and electron donors in water. Such a
136 model could be useful for the management of natural environments, particularly to estimate
137 denitrification rates in groundwater for long-term groundwater protection or for the
138 implementation of corrective measures to decrease the impact of diffuse sources. We describe
139 here a versatile model that does not oversimplify the biogeochemical system (overall reaction
140 of nitrate to N_2) and is suitable for denitrification catalyzed by different microbial consortia.
141 This model includes a multi-step denitrification process that enables better control of the
142 numerous thermokinetic parameters involved by considering all reaction products. This model
143 tests the suitability of the Jin and Bethke approach for each individual mechanism (the
144 “driving forces” of each process). It defines the limiting and weight parameters and we use it
145 to investigate how natural consortia influence the dynamics of denitrification. The model also
146 enables integration of different microbial communities having specific influence on
147 denitrification process. This model allows for evaluation of the relationship between
148 anabolism and catabolism for the heterotrophic micro-organisms under consideration and it
149 enables estimation of the fraction of denitrification that is caused by autotrophic and/or
150 heterotrophic bacteria.

151

152 This work is based on laboratory denitrification experiments (batch and packed bed column
153 done with inoculum from groundwater that contains both heterotrophic and autotrophic
154 bacteria), and yields numerical simulations of the biogeochemical reactions involved in the
155 denitrification processes. Its objectives were to (i) identify the main steps that control the
156 kinetic rate of the denitrification process, (ii) highlight an approach using both batch and
157 flow-through column experiments, (iii) characterize the role played by micro-organisms
158 during each reaction, and (iv) develop a comprehensive biogeochemical model of
159 denitrification.

160

161

162

163

164

165

166 2. Experiments and Modelling

167 2.1 Experimental approach

168 2.1.1 Choice of experimental conditions

169 Denitrification experiments conducted in this study were done with water and rock samples
170 collected in the Coët-Dan catchment, 70 km SW of Rennes (Brittany), in western France,
171 where low nitrate concentrations in groundwater have been attributed to advanced
172 denitrification mechanisms (Pauwels et al., 2001, 2010). The presence of pyrite in the aquifer
173 rock contributes to a high-rate denitrification reaction (Pauwels et al., 1998) mediated by
174 autotrophic bacteria according to the simplified reaction:

175



177

178 Heterotrophic denitrification involving organic matter has, however, also been reported
179 (Pauwels et al., 2001, 2004).

180

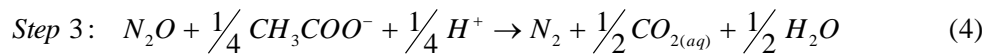
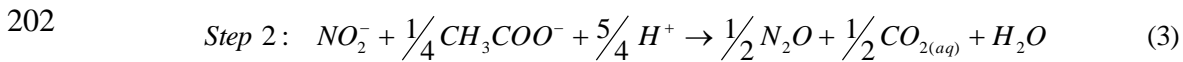
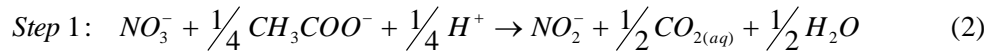
181 Groundwater was collected with a submersible pump and stored in a sterile vessel after three
182 well volumes of water had been purged. The well enabled the collection of water at a depth
183 between 7 and 15 m – a redox zone where there is denitrification (Pauwels et al., 2001).
184 Aliquots were filtered through 0.45 µm pore size for chemical analysis. Aliquots for cation
185 measurements were acidified to pH 2. Alkalinity was measured by titration with HCl. Major
186 cation (Na^+ , K^+ , Ca^{2+} and Mg^{2+}) and anion (NO_3^- , NO_2^- , Cl^- and SO_4^{2-}) concentrations were
187 measured by HPLC, and total iron by spectrophotometry. Dissolved organic C was measured
188 by pyrolysis at 680 °C with CO_2 infrared detection (TOC 5000 Shimadzu).

189

190 The bacterial analysis done on a raw groundwater sample with the “Most Probable Number”
191 method (Halvorson and Ziegler, 1933) confirmed the presence of (i) heterotrophic denitrifying
192 bacteria, (ii) *Thiobacillus denitrificans* (about 2,500 cells mL^{-1}) and (iii) *Acidithiobacillus*
193 *ferrooxidans* (fewer than 0.5 cells mL^{-1}). Most of the population is able to reduce nitrate to
194 nitrite (about 5,870 cells mL^{-1}), whereas only a small fraction is able to reduce nitrate to N_2
195 (about 130 cells mL^{-1}).

196

197 Only heterotrophic denitrification was considered for batch experiments, whereas by using
 198 schist, both heterotrophic and autotrophic processes were involved during the flow-through
 199 column experiment. Experiments were done in the presence of acetate (model organic
 200 compound). This enabled us to break down the global mechanism and quantify the kinetics of
 201 the various denitrification steps (Eqs. 2 to 4).



203 2.1.2 Batch experiments

204 Batch assays were done in glass serum flasks (500 mL) supplemented with 150 mL (biotic
 205 flasks) or 300 mL (abiotic flasks) of sampled groundwater (Table 1). The headspace was
 206 flushed with CO₂ gas to remove oxygen from the flasks. CO₂ was chosen instead of N₂ or
 207 CO₂ + N₂ mixtures in order to avoid a secondary nitrogen source in a nitrogen-enriched
 208 medium. The flasks were sterilised by autoclaving at 120 °C for 20 minutes. The biotic flasks
 209 were inoculated with 150 mL of non-sterile groundwater. Six flasks were prepared – 3 biotic
 210 flasks and 3 abiotic flasks. Ten millilitres (10 mL) of a 3,000-mg KNO₃ L⁻¹ solution were
 211 added to the medium to give a final concentration of 50 mg NO₃⁻ L⁻¹ and 50 mL of a 1476.4-
 212 mg Na₂CH₃COO L⁻¹ solution were added to give a final concentration of 50 mg acetate L⁻¹. A
 213 trace-element solution (0.25 mL) containing the following, in mg L⁻¹, was added to this:
 214 EDTA, 500; MnSO₄, H₂O, 2.6; FeSO₄, 200; ZnSO₄, 7 H₂O, 10; H₃BO₃, 30; CoCl₂, 6 H₂O, 20;
 215 CuCl₂, 2 H₂O, 1; NiSO₄, 7 H₂O, 2.4; and Na₂MoO₄, 2 H₂O, 3.

216 Water and gas samples were collected at regular intervals to monitor the reaction.

217 2.1.3 Flow-through column experiment

218 Denitrification was studied in a glass column (0.45 L) equipped with an external water jacket
 219 that maintained the temperature at 14 °C throughout the experiment (Fig. 1). The column had
 220 an internal diameter of 3.5 cm and was 32 cm high. It was packed with 599.3 g of crushed
 221 schist (200 µm, see Table 2 for mineralogical assemblage) and sterilised 3 times at 24-hour
 222 intervals by autoclaving for 1 hour at 121 °C.

223 After sterilisation, the column was inoculated with a denitrifying bacteria consortium
224 specially prepared for this experiment. The enrichment culture, prepared with a groundwater
225 sample, was made up in sterile 500 mL serum flasks containing a culture medium composed
226 of 150 mg L⁻¹ of KNO₃, 5.66 mg L⁻¹ of Na-acetate and 1 mL of the trace-element solution
227 described above. The pH of the medium was adjusted to 6.5 with a 1 molar H₂SO₄ solution.
228 The serum flasks were then flushed with N₂ gas to ensure anaerobic conditions. The
229 enrichment culture was incubated for 3 weeks at 14 ± 2 °C. Aliquots were sampled
230 periodically to monitor bacterial growth and the nitrate concentration in the flask.

231

232 The experiment was done with synthetic water prepared with chemicals reagents (Table 3).
233 The nitrate-bearing solution was injected into the column after the inoculum solution for 200
234 hours in two phases:

- 235 - Phase 1 (between 0 and 100 hours). The column was fed continuously with synthetic
236 solution 1 (Table 3) in the up-flow mode by an adjustable peristaltic pump (flow rate =
237 0.25 mL min⁻¹). The major element concentrations in the injected aqueous solution
238 were similar to those of the groundwater (Table 1). Before it was injected into the
239 column (Fig. 1), the synthetic medium was continuously sparged with CO₂ gas and
240 placed in a thermostatic chamber (14°C).
- 241 - Phase 2 (between 100 and 200 hours). A carbon source (acetate) with a concentration
242 of 10 mg C L⁻¹ (Table 3) was added to the synthetic solution 2.

243 An automatic sampler (Gilson) was connected to the outlet column in order to periodically
244 collect water samples.

245 The hydrodynamic characteristics of the column were determined by injecting a conservative
246 tracer, NaBr, before the denitrification experiment began. A pulse of the tracer at a constant
247 flow rate (0.25 mL min⁻¹) was injected and the outlet concentration of bromide was monitored
248 with time. Based on the bromide breakthrough curve, the mean residence time was estimated
249 to be 12.5 hours. The dispersivity coefficient, 0.02 m, was determined by modelling the flow
250 transport with PHREEQC (Parkhurst and Appelo, 1999). A pore volume of 190 cm³,
251 corresponding to a mean porosity of 35 %, was calculated from the residence time and the
252 injection flow rate.

253

254

255 **2.1.4 Analytical procedure**

256 Nitrate, nitrite and acetate concentrations were determined during the batch and flow-through
257 column experiments by ion chromatography with a DIONEX IC3000-SP-EG-DC system
258 equipped with an AS50 autosampler and a conductimetric detector. A gradient elution with
259 sodium hydroxide, from 10 to 100 mM, was applied at 1 mL min⁻¹ at 30 °C through an
260 anionic column (DIONEX-AG19 and AS19 HC, 4 mm ID). An aliquot was sampled for
261 bacteria counting using a Thoma cell by optic microscopy (Zeiss 400x). N₂O in gas samples
262 was analysed with a chromatograph (VARIAN 3800) equipped with a gas injection valve and
263 an electron capture detector.

264
265 For the flow-through column experiment, the samples were collected in glass tubes previously
266 flushed with nitrogen and sealed. The tubes were opened in an anaerobic glove box for
267 analyses. One aliquot of raw sample was used for bacteria counting. pH and oxido-reduction
268 potential (ORP) were measured on the raw sample and the remaining water was filtered at
269 0.45 µm for anionic analyses (NO₃⁻, NO₂⁻, SO₄²⁻, Cl⁻, CH₃COO⁻) by ion chromatography.

270

271 **2.2 Numerical modelling approach**

272 Micro-organisms affect the geochemical cycle of many chemical species by catalysing
273 chemical reactions while the physicochemical properties of the environment control the
274 activities of micro-organisms by providing habitats, nutrients, and energy (Jin and Bethke,
275 2007). Physicochemical, thermodynamic/kinetic and biological phenomena must, therefore,
276 be accurately predicted before we can determine the fate of chemical species (reactants and
277 products), microbial population activity and microbial growth. Modelling requires a robust
278 numerical model able to account for all of these strongly linked characteristics and the
279 evolving properties.

280 **2.2.1 Thermodynamic and biological coupling**

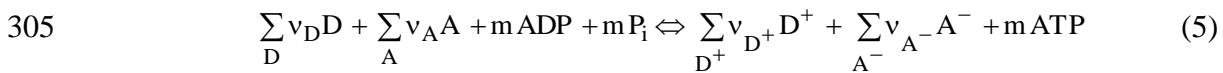
281 Various kinetic rate laws and coupled models have been proposed to describe the thermo-
282 kinetics of bacterial growth (Hoh and Cord-Ruwisch, 1996; Fennel and Gossett, 1998; Hunter
283 et al., 1998; Noguera et al., 1998; Kleerebezem and Stams, 2000; Knab et al., 2008). They are
284 all based on Monod's equation and often add terms containing a thermodynamic factor (such
285 as the reaction quotient Q/K, where Q is the ionic activity product and K is the equilibrium

286 constant of the reaction) or a minimum free energy (ΔG_{\min}). However, most of these
 287 approaches were developed to describe specific physiological systems with constant ΔG_{\min}
 288 values. The approach proposed by Jin and Bethke (2002, 2003, 2005, 2007) goes further and
 289 seems to be more suitable and flexible because it associates (i) a kinetic factor for an electron
 290 donor, (ii) a kinetic factor for an electron acceptor, (iii) a term for bacterial growth, and (iv) a
 291 thermodynamic factor. Furthermore, the Jin and Bethke approach makes it possible to propose
 292 a consistent reactive transport model for hydro-geochemical systems with kinetically
 293 dissolving/precipitating minerals for which the reaction quotient Q/K is used in the context of
 294 the Transition State Theory (Lasaga, 1984; Palandri and Kharaka, 2004).

295

296 The Jin and Bethke approach is based on the relationship between chemical redox reactions
 297 and microbial growth under natural conditions. Redox reactions, which are often slow, can, in
 298 some rare cases, be at thermodynamic equilibrium or close to it (Lindberg and Runnels, 1984;
 299 Keating and Bahr, 1998; Michard, 2002; Stefansson et al., 2005). In natural systems, the
 300 progress of redox reactions is usually catalysed by micro-organisms. During this process,
 301 bacteria use some of the released energy to synthesize adenosine triphosphate (ATP) from
 302 adenosine diphosphate (ADP) and the orthophosphate ion (intracellular PO_4^{3-} , denoted P_i)
 303 (Eq. 5):

304



306 where v_{D} , v_{A} , v_{D^+} and v_{A^-} are the stoichiometric coefficients of chemical species (D = donor,
 307 A = acceptor). The ATP serves as a chemical energy reserve (stock).

308

309 From this, Jin and Bethke (2002) derived a comprehensive kinetic law (Eq. 6) that can
 310 account quantitatively for the thermodynamic driving force of redox reactions:

311

$$312 \quad v = k[X] F_{\text{D}} F_{\text{A}} F_{\text{T}} \quad (6)$$

313

314 where v is the overall rate of microbial respiration ($\text{mol L}^{-1} \text{s}^{-1}$), k is the intrinsic kinetic
 315 constant ($\text{mol g}^{-1} \text{s}^{-1}$) and $[X]$ is the biomass concentration (g L^{-1}). F_{D} and F_{A} (ranging from 0
 316 to 1, dimensionless) are kinetic factors accounting for the effects of the concentration of
 317 dissolved chemical species involved in redox reactions (Eqs. 7 and 8):

318
$$F_D = \frac{\prod [D]^{\beta_D}}{\prod [D]^{\beta_D} + K_D \prod [D^+]^{\beta_{D^+}}} \quad (7)$$

319
$$F_A = \frac{\prod [A]^{\beta_A}}{\prod [A]^{\beta_A} + K_A \prod [A^-]^{\beta_{A^-}}} \quad (8)$$

320 where β_D , β_A , β_{D^+} , β_{A^-} are exponents of reactant and product concentrations. Their values are
 321 not predicted by theory and depend on details of the electron transport mechanism (Jin and
 322 Bethke, 2003). K_D and K_A are constants for electron donor D and acceptor A.

323

324 F_T (ranging from 0 to 1, dimensionless) is the thermodynamic potential of the overall reaction
 325 corresponding to the driving force of the reaction (Eq. 9):

326

327
$$F_T = 1 - \exp\left(\frac{\Delta G_{\text{redox}} + m \Delta G_P}{\chi RT}\right) \quad (9)$$

328

329 where ΔG_{redox} is the free enthalpy of the reaction, ΔG_P is the phosphorylation energy, and χ is
 330 the average stoichiometric coefficient of the overall reaction. The coefficient m is the number
 331 of synthesised ATP defined in the overall reaction (Eq. 5).

332 2.2.2 Numerical modelling approach

333 The Jin and Bethke approach was included in the geochemical code PHREEQC (Parkhurst
 334 and Appelo, 1999) to deal with denitrification in the presence of acetate. This approach
 335 requires, however, that the database used by the calculation code be modified. In its standard
 336 use, this code is based on chemical equilibrium calculations of aqueous solutions interacting
 337 with minerals and gases using general and extended thermodynamic databases, and aqueous
 338 redox reactions are considered to be at equilibrium. As this is rarely the case (Stefansson et
 339 al., 2005), a kinetic term must be introduced for redox reactions. PHREEQC is a very flexible
 340 code for simulating chemical reactions in the aqueous phase and enables the re-writing of
 341 aqueous redox reactions to account for kinetic constraints. Since this study focuses on nitrate
 342 behaviour, all redox reactions involving nitrogen were re-written to take into account the
 343 kinetics of successive transformations (decreasing redox number: $N(V) \rightarrow N(III) \rightarrow N(II) \rightarrow N(I)$
 344 $\rightarrow N(0)$). The chemical equilibria between nitrate-nitrite- N_2O and N_2 were removed from the

345 database and replaced by kinetic laws. Only aqueous complexing reactions of nitrate and
346 nitrite with cations and vapour-liquid equilibrium for N₂O and N₂ were kept.

347 **2.2.3 Thermo-kinetic simulation of denitrification processes**

348 The coupled thermodynamic-biogeochemical approach is applied to the reduction of (i) nitrate
349 to nitrite (Eq. 2), (ii) nitrite to nitrous oxide (Eq. 3) and (iii) nitrous oxide to nitrogen (Eq. 4).
350 These reactions are kinetically constrained, whereas thermodynamic equilibria are retained
351 between all other species in the aqueous phase including nitrogen species (ligand) complexing
352 cations. The term F_T in Eq. (9) was determined based on the following assumptions. The
353 phosphorylation enthalpy (ΔG_p) is roughly estimated to be 50 kJ mol⁻¹ under typical
354 physiological conditions (White, 1995), whereas χ and m are reaction-dependent parameters.
355 For Eq. (2), $\chi = 2$ and $m = 2/3$. Two protons are transferred by electron pairs and three are
356 required for ATP synthesis (Jin and Bethke, 2005). For Eqs. (3) and (4), few data are
357 available in the literature. Consequently, the same values for χ and m were used for the three
358 reactions (Eqs. 2 to 4) (Q. Jin, personal communication, August 2009). Gibbs free enthalpies
359 of each reaction (ΔG_{redox}), determined at each time step from the free standard enthalpy of
360 each reaction are -140.12 kJ mol⁻¹, -248.92 kJ mol⁻¹ and -314.43 kJ mol⁻¹ for Eqs. (2) to (4),
361 respectively (Michard, 2002).

362

363 In Eqs (7) and (8), the functions $K_D \cdot \prod_{D^+} [D^+]^{\beta_{D^+}}$ and $K_A \cdot \prod_{A^-} [A^-]^{\beta_{A^-}}$ are kinetic terms that
364 replace the half-saturation constant in the Monod equation. In a first approximation, the
365 kinetic term can be expected to be equivalent to the half-saturation constant only when the
366 thermodynamic potential is close to 1 (Jin and Bethke, 2005) or when, under appropriate
367 geochemical conditions such as when the pH is buffered, there is a large substrate
368 concentration and no build-up of metabolic products (Jin and Bethke, 2007). In this study, as
369 demonstrated below, the pH is buffered and the thermodynamic factor is close to 1 throughout
370 the reaction. Consequently, the two kinetic terms are replaced by two half-saturation constants
371 (K'_D and K'_A). For step 1 of denitrification (Eq. 2), the values used are from Clément et al.
372 (1997): $K'_D = 1.20 \text{ mg L}^{-1}$ and $K'_A = 0.66 \text{ mg L}^{-1}$. As no data are available for nitrite (Step 2 –
373 Eq. 3) or N₂O (Step 3 – Eq. 4), we used the same values for K'_A and K'_D as those determined
374 for nitrate.

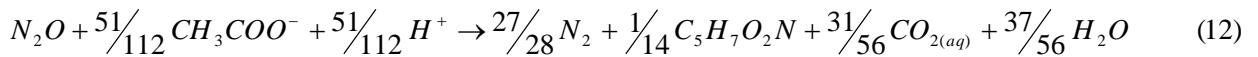
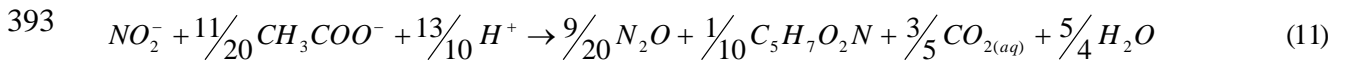
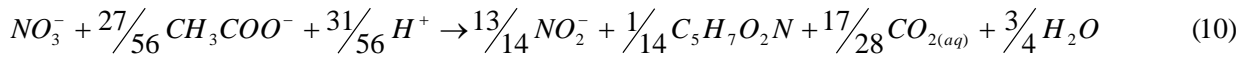
375

376 A growth yield of 0.13 mg-biomass/mg-NO₃⁻ (Clément et al., 1997) was used for step 1 (Eq.
377 2). For steps 2 and 3 (Eqs. 3 and 4), Clément et al. (1997) did not give a value for growth
378 yields. Values found in the literature indicate that the growth yield for nitrite is about three
379 times that for nitrate (Peyton et al., 2001): a value of 0.40 mg-biomass/mg-NO₂⁻ was therefore
380 used. For nitrous oxide, as no literature data were found, the same value as the one for nitrate
381 was chosen arbitrarily (0.09 mg-biomass/mg-N₂O). For calculations, a conversion factor of
382 6.2 10⁹ cells mg⁻¹ biomass was used to convert experimental data (in cells mL⁻¹) to input data
383 for numerical model (in mg-biomass mL⁻¹) (Clément et al., 1997).

384

385 Because denitrification by heterotrophic bacteria is studied, the model must also take into
386 account the microbial growth using carbon from acetate and nitrogen from each nitrogen-
387 bearing species in solution. For the numerical simulations, the biomass is represented using a
388 simplified generic form (C₅H₇O₂N) and integrated into Eqs. (2) to (4). The growth yield
389 determined above provides information concerning the stoichiometry of the reaction, i.e. the
390 number of moles of biomass synthesised from nitrate, nitrite and nitrous oxide consumption.
391 Consequently, Eqs. (2) to (4) are rewritten:

392



394

395

396 These stoichiometric equations, which take into account the biomass growth (anabolism),
397 were incorporated in the geochemical code. Although bacterial death obviously also affects
398 the micro-organism population during the experiments, it was disregarded. We assumed that
399 no significant nutrients (or chemical components) coming from dead bacteria are released into
400 solution.

401

402

403 3. RESULTS AND DISCUSSION

404 3.1 Batch experiments

405 3.1.1 *N*-species

406 Batch experiments focused on measuring kinetic parameters for the entire denitrification
407 reaction, from nitrate to N₂. The abiotic flasks used as blanks show no denitrification during
408 the entire experimental time. We know, therefore, that the nitrate attenuation observed in the
409 biotic flasks is due to biological rather than chemical processes.

410

411 The results obtained on biotic flasks indicate a total denitrification in 40 days. Each
412 experiment began with a period of about eight days during which the nitrate concentration did
413 not vary (Fig. 2). Under our experimental conditions, micro-organisms seem to need time to
414 adjust before denitrification begins. Nitrate reduction starts after 8 days with a decrease in
415 nitrate correlated with the formation of nitrite in solution.

416

417 This first nitrate reduction reaction lasts about 30 days. At this time, nitrogen (+V) has been
418 completely reduced to nitrogen (+III) and nitrite is the major aqueous nitrogen species. Only
419 small and transitory amounts of N₂O are found in solution. Significant quantities of this
420 species appear in solution when nitrite begins to be reduced by micro-organisms. The N₂O
421 concentration then increases steadily before N₂ appears and nitrogen(I) is finally reduced to
422 nitrogen(0).

423

424 Modelling is based on experimental constraints and the results obtained, using the Jin and
425 Bethke approach, are described above. The kinetic constants for each reaction are:

- 426 - Nitrate to nitrite: An initial period (day 0 to day 8) during which no measurable microbial
427 activity and no denitrification is recorded, is followed by a second period (day 8 to day 29)
428 during which nitrate is reduced to nitrite consistent with a mean kinetic constant of $4.6 \cdot 10^{-7}$
429 mol N L⁻¹ h⁻¹.
- 430 - Nitrite to nitrous oxide: A first period (day 0 to day 29), up to complete nitrate reduction,
431 during which the nitrite reduction rate is assumed to be nil, is followed by a second period
432 (day 30 to day 40) during which the nitrite reduction rate is about $2.3 \cdot 10^{-7}$ mol N L⁻¹ h⁻¹.

433 - Nitrous oxide to nitrogen: The kinetic rate is highly dependent on nitrate and nitrite
434 concentrations. Up to the total reduction of nitrate (day 0 to day 29), the nitrous oxide
435 reduction rate is assumed to be nil, whereas thereafter (day 29 to day 60), a value of
436 $2.1 \cdot 10^{-7} \text{ mol N L}^{-1} \text{ h}^{-1}$ provides a rather good fit of the observed results.

437 By coupling batch experiments and numerical modelling we were able to define the different
438 steps of the denitrification process and determine the respective kinetic rates. The kinetic rate
439 for the first reduction step (nitrate to nitrite) falls within the range reported in the literature
440 (from $5.0 \cdot 10^{-7}$ to $2.0 \cdot 10^{-6} \text{ mol-N L}^{-1} \text{ h}^{-1}$) for denitrification with organic matter (Star and
441 Guillham, 1993; Schipper and Vojvodic Vukovic, 1998, 2000; Devlin et al., 2000). This
442 experiment shows that the reduction of nitrite (and the formation of nitrous oxide) is related to
443 nitrate consumption. As long as nitrate is present, nitrite increases and is measurable in
444 solution. In natural environments, high nitrite concentrations are rarely observed, except in
445 specific cases (Kelso et al., 1999). In laboratory systems, this nitrite accumulation is often
446 observed by the use of acetate as the electron donor. Carbon sources such as acetate and
447 propionate cause nitrite to accumulate in the medium, which does not occur with butyrate,
448 valerate or coproate (Wilderer et al., 1987; van Rijn and Tal, 1996). These authors assume
449 that in the presence of acetate, nitrite accumulation is caused by differences in nitrate and
450 nitrite reduction rates and by the competition between nitrate and nitrite reduction pathways
451 for electrons. Our experiments confirm this hypothesis of competition between the two
452 reduction processes in the presence of acetate – nitrite reduction does not start until all of the
453 nitrate has been consumed, favouring nitrate reduction before nitrite reduction and the nitrite
454 accumulation.

455 *3.1.2 pH pattern*

456 The pH is initially stable or decreases slightly (during nitrate reduction to nitrite, up to day
457 29), and then increases during nitrite reduction (day 29 to day 40, Fig. 3). Calculated pH
458 values fit the experimental data relatively well and the major trends are reproduced, except for
459 some small discrepancies in the first part of the experiment. During nitrate reduction (Eq. 2), a
460 small increase in pH is predicted by numerical calculations due to proton consumption,
461 whereas experimental data show a slight decrease. The slopes of the curves for observed and
462 simulated results are identical for the nitrite reduction reaction. Eq. (3) indicates that the
463 proton consumption is higher than in the previous nitrate reduction reaction – the
464 consequence of this being a change in the slope with a relatively greater increase in pH

465 between day 30 and day 40. However, pH does not vary greatly due to the buffering capacity
466 of the reactive aqueous solution.

467 *3.1.3 Acetate as the electron donor*

468 Acetate is the electron donor used by micro-organisms to promote the heterotrophic
469 denitrification reaction. The concentration is constant during the first 8 days (when no nitrate
470 is consumed) and then decreases sharply (Fig. 4). After 40 days, there is no longer any acetate
471 (for 2 of the 3 replicates). The simulation correctly fits the observed data, except for one of
472 the replicates, for which no explication can be found, since all of the other measured variables
473 (nitrogen species concentration, pH, biomass concentration) are consistent for the three
474 replicates. Numerical simulations confirm that all of the acetate is consumed during the
475 experiment. It is used to synthesize CO₂ (catabolism) and biomass (anabolism) (Eqs. 10 to
476 12). When numerical modelling was done without taking the bacteria anabolism into
477 consideration (Fig. 4 - dashed line) only about 30 mg of acetate are used to reduce 50 mg of
478 nitrate (Eqs. 2 to 4).

479 Acetate is the source of both the electrons and the carbon needed by bacteria to proliferate.
480 This is highlighted by the two simulations. One considers only catabolism, while the other
481 takes into account both the anabolism and the catabolism of the micro-organisms (Fig. 4).
482 Results using the first scenario do not match the measured acetate concentrations, whereas
483 those using the second scenario agree with the observed acetate consumption data. This
484 second scenario indicates that about 40 % of the carbon from acetate is used for anabolism
485 and 60 % is used for catabolism. From Eqs. (10) to (12), the calculated mass-balance confirms
486 that 41 % of the carbon coming from acetate is used for biomass production, in agreement
487 with literature data. For aerobic degraders, Greskowiak et al. (2005) proposed a value of 60 %
488 for anabolism, meaning that 40 % of the carbon is converted to CO₂. However, for anaerobic
489 denitrification in the presence of acetate, this ratio is reversed. Clément et al. (1997) defined a
490 biomass growth yield of about 20 %, whereas Odenchantz et al. (1990) and Istok et al. (2010)
491 have proposed values of 37.5 % and 41 %, respectively.

492 *3.1.4 Biomass growth*

493 Fig. 5 shows the evolution of the biomass in the batch experiment. The bacterial population
494 increases rapidly (day 0 to day 8) before decreasing and then increasing once again. It
495 stabilizes after 40 days (i.e. the end of nitrite reduction). The bacterial growth model, based
496 on nitrate, nitrite and nitrous oxide reduction, produces results that are in relatively good

497 agreement with experimental data. The overall trend and the final biomass concentration are
498 in agreement with observed data. The only discrepancy concerns the first period (day 0 to day
499 8). Some bacterial activity, independent of the denitrification process since nitrate reduction
500 and acetate oxidation are nil (or extremely low) during this period, is assumed to influence the
501 biomass population and probably pH during this period. The batch experiments were done
502 with groundwater initially containing both heterotrophic and autotrophic bacteria. Autotrophic
503 bacteria (very active in the field) might develop during the experiment in the aqueous
504 solution. These use the mineral carbon (bicarbonate), and their activity might explain the
505 biomass peak and the slight decrease in pH (Fig. 3). This is hypothetical, however, and since
506 it does not play a major role in the overall denitrification process, it was disregarded in the
507 numerical calculations.

508 The measurements of biomass concentration in the three replicates also show that the
509 bacterial growth stabilizes after 40 days, in correlation with the total consumption of electron
510 donors and acceptors. Acetate and nitrate – rather than the bioavailability of other elements –
511 seem to be the limiting factors of bacterial activity. As an example, a simple calculation of the
512 amount of phosphorus needed shows that, assuming a classical formulation
513 $\Delta C:\Delta N:\Delta P \approx 106:16:1$ for dry biomass (Sigg et al. 2000), a few $\mu\text{mol P L}^{-1}$ are necessary to
514 generate the concentrations of biomass measured in the three replicates. The calculated P
515 concentration and the limit of quantification have the same order of magnitude. We therefore
516 assume that the natural groundwater used for these experiments provides enough trace
517 elements (such as phosphorus) for the growth of the bacterial community.

518 *3.1.5 Remarks on the Thermodynamic Potential Factor*

519 One objective of this study was to determine the relative weight of kinetic factors influencing
520 global denitrification. The thermodynamic potential factor (F_T) remains constant (and equal to
521 1) throughout the experiment (Figs. 6 and 7). For denitrification in the presence of acetate, the
522 thermodynamic factor has no affect on denitrification. For step 1 (i.e. reduction from nitrate to
523 nitrite – Eq. 2), the denitrification process is governed by the kinetic factor (F_A) related to the
524 electron acceptor concentration (i.e. nitrate), whereas for step 2 (i.e. reduction from nitrite to
525 nitrous oxide – Eq. 3), the kinetics of denitrification is limited by F_A (i.e. nitrite concentration)
526 and mainly F_D factors (i.e. acetate concentration). For denitrification in the presence of acetate
527 (Figs. 6 and 7), the thermodynamic factor can be disregarded and the global kinetics of
528 denitrification are governed mainly by the concentrations of electron donors/acceptors. The

529 model proposed by Jin and Bethke is, however, entirely suitable for simulating bacteria-
530 mediated changes in the redox state of a complex biogeochemical system.

531 **3.2 Flow-through column experiment**

532 Flow-through column experiments should help us better understand the influence of flow on
533 water chemistry, in particular on the denitrification process. Tarits et al. (2006) have
534 demonstrated the influence of hydrodynamic factors on water chemistry. They point out that
535 denitrification is activated by pumping in the aquifer. In columns and, more generally, in
536 consolidated porous media, microbial communities can also develop in biofilms, creating
537 locally variable redox conditions and processes (Yu and Bishop, 1998; Bishop and Yu, 1999).
538 Our column experiment provides an opportunity to observe whether the denitrification kinetic
539 rates determined using batch experiments are always valid and can be used as is in transport
540 experiments. The breakthrough curves for nitrate and nitrite are given in Fig. 8 and for
541 chloride and sulphate in Fig. 9.

542 The nitrate concentration increases until it reaches a constant value equal to the input
543 concentration (50 mg L^{-1}). The nitrite concentration is lower than 2 mg L^{-1} (Fig. 8). The
544 synthetic solution 1 (Table 3) has lower chloride and sulphate concentrations than the
545 inoculum solution initially introduced in the column. This explains the decrease in the outlet
546 concentrations of these two ions during the first hours of the experiment (Fig. 9). Between 50
547 and 100 hours, the outlet concentrations for chloride, sulphate and nitrate are the same as the
548 inlet concentrations: the system reaches a steady state. No denitrification occurs in the column
549 during this period despite the presence of bacterial inoculum in the system and of pyrite in the
550 schist (Table 2).

551

552 At time = 100 hours, phase 2 of the experiment begins with the input of a carbon source. A
553 solution containing nitrate (50 mg L^{-1}), acetate (10 mg L^{-1}) and sulphate (33.78 mg L^{-1}) is
554 injected into the column (synthetic solution 2, Table 3). The nitrate concentration at the outlet
555 of the column decreases immediately and the nitrite concentration increases. About 50 % of
556 the injected nitrate has been reduced to nitrite and to reduced nitrogen species after 190 hours
557 (Fig. 8). Nitrate removal is not in a steady state. It is more rapid between 100 and 130 hours
558 than during the period between 130 and 200 hours. Nitrite concentrations followed the
559 opposite trend with a sharp increase between 100 and 130 hours and a smoother variation
560 thereafter (130 to 200 hours). The chloride concentration does not vary when the injected

561 solution changes, whereas the sulphate concentration does. Since synthetic solution 2 contains
562 less sulphate than synthetic solution 1, a decrease in the sulphate concentration was expected.
563 Although a small drop was observed, the outlet concentration of this species was always
564 greater than the injected concentration, as opposed to what occurred during the previous phase
565 (0 to 100 hours). Sulphates are therefore produced within the column, and we conclude that
566 dissolved sulphates come from an interaction between the aqueous solution and minerals.
567 Considering the mineralogical assemblage of the constituting rock (pyrite-bearing schist), the
568 sulphur production is attributed to the dissolution/oxidation reaction of pyrite. During this
569 stage (100 to 200 hours), two electron donors impact on the denitrification process – acetate
570 (Eqs. 2 to 4) and pyrite (Eq. 1).

571 Based on the results of the column experiment, we assume that the bacterial inoculum used to
572 colonize the schist was composed mainly of heterotrophic bacterial species. The specific
573 medium, enriched in acetate and used to develop this inoculum, probably favours the growth
574 of heterotrophic bacteria (Tranvik and Höfle, 1987), which have a specific growth rate higher
575 than that of autotrophic micro-organisms (Tsai and Wu, 2005). Marchand and Silverstein
576 (2002) also show that heterotrophic microbial growth could have an impact on the behaviour
577 of autotrophic populations, in particular on the biological oxidation of pyrite. They suggest
578 that the development of heterotrophic micro-organisms might inhibit the rate and the extent of
579 sulphide mineral oxidation. This experiment highlights the major role played by heterotrophic
580 bacteria in the denitrification process since it is initiated by the addition of organic matter to
581 the injected solution.

582 The absence of denitrification due to the oxidation of pyrite by nitrate during the first period
583 (0 to 100 hours) was not expected since microbial denitrification had been observed at the site
584 where the samples were collected (Pauwels et al., 1998). However, these authors did not
585 specify whether the autotrophic micro-organisms were chemolithotrophic bacteria (which use
586 inorganic carbon as a carbon source and non-carbon compounds as an electron source,
587 Chapelle 2001) or chemoorganotrophic bacteria (which use inorganic carbon as a carbon
588 source and carbon compounds as an electron source, Chapelle 2001). From field
589 measurements, they simply identified the preponderant role of autotrophic bacteria compared
590 to that of heterotrophic bacteria. The results of our experiment show that chemoorganotrophic
591 bacteria had been fostered by the acetate-enriched medium used to develop the inoculum,
592 whereas chemolithotrophic bacteria, probably present in the inoculum but in low numbers,
593 were not active enough to initiate the denitrification process. Consequently, the low

594 population of chemolithotrophic micro-organisms and the absence of organic matter for
595 chemoorganotrophic bacteria prevented any decrease in the nitrate concentration during this
596 first period.

597

598 The column experiment was modelled with PHREEQC using a 1D column (discretised into
599 10 sections, each 3 cm long) with hydrodynamic characteristics determined using the bromide
600 tracer (see paragraph 2.1.2). The simulation complies with the two-phase experiment:
601 injection of a nitrous solution without organic carbon (synthetic solution 1, Table 3) during
602 the first 100 hours, followed by injection of a nitrate/acetate solution (synthetic solution 2,
603 Table 3) from hour 100 to hour 200. A constant injection flow rate is imposed at the inlet of
604 the column and a Cauchy boundary condition is assumed at the outlet. A biomass
605 concentration of $1.6 \cdot 10^7$ cells mL^{-1} is assumed at the beginning at the experiment.

606 For the biogeochemical part of the simulation, the kinetic parameters determined in batch
607 systems with acetate were used without modification (Eqs. 10 to 12). However, in this flow-
608 through column experiment, the kinetic rate for reaction 1 (i.e. pyrite oxidation, Eq. 1) had to
609 be estimated ($3.2 \cdot 10^{-7}$ mol N L^{-1} h^{-1}) based on field data (Postma et al., 1991; Pauwels et al.,
610 1998). To our knowledge, there is no literature data for the parameters used to calculate the
611 thermodynamic factor of reaction 1 (Eq. 1). Only the free enthalpy can be calculated: -456 kJ
612 mol^{-1} (Michard, 2002). This value is high (of the same order of magnitude as that of acetate),
613 and in batch experiments it was demonstrated that the thermodynamic factor is close to 1 with
614 such a high ΔG_0 . In a first approximation, for this calculation, the thermodynamic factor is
615 assumed to be 1. A Monod approach is then used for reaction 1 (Eq. 1). This is justified due to
616 the high free enthalpy of the reaction and the excess of pyrite in the schist (Pauwels et al.,
617 1998).

618 The kinetic rates used for each reaction make it possible to reproduce the experimental values
619 for nitrate, nitrite (Fig. 8) and sulphate (Fig. 9). The outlet sulphate concentrations, calculated
620 from the inlet SO_4 concentration and the number of moles of pyrite oxidized by nitrates
621 (Reaction 1, Eq. 1), are in good agreement with the observed data (Fig. 9). A small difference
622 between measured and calculated sulphate concentrations is observed at 120 hours. Numerical
623 modelling predicted a small peak in sulphate that is not observed. In the column experiment,
624 the autotrophic bacteria have a short time lag, which is not considered in the numerical
625 approach since the two bacterial processes (heterotrophic and autotrophic) are activated at the

626 same time. This simultaneous activation might explain the punctual over-estimation of the
627 sulphate concentration.

628 The numerical simulation of the second part of the experiment (between 100 and 200 hours)
629 also confirms that the bacteria active in the column are, for the most part, heterotrophic since
630 the outlet nitrate concentration starts to decrease when acetate is co-injected with nitrate.
631 However, heterotrophic denitrification alone cannot explain the measured decrease in the
632 nitrate concentration. Autotrophic denitrification must also be involved to match the observed
633 data. The two autotrophic processes (chemoorganotrophic and chemolithotrophic) are also
634 assumed to be active in this experiment. Indeed, the addition in the injected solution of a
635 carbon source (acetate) can activate the chemoorganotrophic mechanism. Moreover,
636 heterotrophic bacteria produce alkalinity (mainly as dissolved CO_2), due to acetate
637 degradation for their catabolism. According to the reactions described in Eqs. (10) to (12), 1
638 mole of nitrate induces the formation of about 1.8 moles of $\text{CO}_{2,\text{aq}}$. This increase in alkalinity
639 could explain the increased activity of chemolithotrophic bacteria. All of these processes are
640 assumed to be active in the column experiment.

641 The absence of any source of organic matter, therefore, prevents the development of
642 chemoorganotrophic activity. The low alkalinity of the injected solution also stops the activity
643 of chemolithotrophic bacteria. With the addition of acetate, the heterotrophic bacteria are
644 activated and produce alkalinity, which is immediately used by chemolithotrophic micro-
645 organisms. We also assume that chemoorganotrophic bacteria are activated by the carbon
646 availability. However, neither the data nor the model can explain the relative weight of each
647 autotrophic community. This simultaneous heterotrophic/autotrophic denitrification has been
648 described for nitrate removal from high-nitrate wastewater (Gommers et al., 1988;
649 Aminzadeh et al., 2010). These authors emphasize the high efficiency of such a treatment,
650 which enables the removal of sulphide, acetate and nitrate in natural and synthetic wastewater
651 in fluidized bed reactors. Oh et al. (2002) calculated that the reduction of 1 mg of nitrate
652 nitrogen, with methanol, generates 3.57 mg of CaCO_3 . According to these authors, the two
653 processes are linked and a lack of any organic source can decrease the performance of
654 denitrification treatment.

655

656 Modelling of both heterotrophic and autotrophic processes correctly reproduces the observed
657 outlet concentrations of nitrate, nitrite and sulphate. The outlet nitrate concentration after 200

658 hours is close to 30 mg L⁻¹ (for an inlet concentration of 50 mg L⁻¹), which means that the two
659 species of bacteria are able to remove about 40 % of the initial nitrate. A comparison of two
660 calculations (results not shown here), one done with and the other without considering the
661 autotrophic mechanism, indicates that 80 % of the nitrate consumption is due to heterotrophic
662 denitrification and the remainder is due to autotrophic processes. The numerical results for the
663 nitrite concentration are in good agreement with the observed data. As the modelling
664 approach considers only the production of nitrite by the heterotrophic process, we deduce that
665 autotrophic denitrification does not release any nitrite into solution (or that the kinetic rate of
666 nitrite production equals the kinetic rate of nitrite consumption). This absence of nitrite
667 accumulation (via pyrite oxidation) has been observed in NO₃⁻-reducing cultures (Van Beer,
668 2000; Weber et al., 2001).

669

670 The experimental results of this flow-through column experiment show no time lag when
671 acetate is injected into the column. In batch experiments, there is no heterotrophic microbial
672 activity during the first 8 days (Fig. 2). In the field, Pauwels et al. (1998) observed an
673 autotrophic metabolic lag of about 40 hours. The absence of a microbial adjustment period
674 can be attributed to the experimental protocol:

675 - During the first phase of the experiment (the first 100 hours), the microbial population was
676 accustomed to a NO₃⁻-containing solution, thus limiting the beginning of microbial activity,
677 when acetate was added.

678 - The flow rate through the column is low compared to the flow rate in field studies where
679 transport processes have a greater impact on denitrification (Pauwels et al., 1998). Moreover,
680 the column experiment is done using crushed schist. Consequently, the exchanges, the contact
681 surface and, therefore, the interactions between aqueous solution, mineral (in particular
682 pyrite) and micro-organisms are probably more favourable, decreasing the time lag.

683

684 **4. CONCLUSIONS**

685 This study focuses on heterotrophic and autotrophic denitrification processes, i.e. the
686 reduction of nitrate (NO₃⁻) to nitrogen (N₂). Although denitrification in soils and aquifers is
687 studied extensively for water quality, diffuse pollution transfer, and remediation, there is still
688 an on-going debate in the scientific community concerning the contribution of organic matter

689 as an electron donor when other mineral electron donors (i.e. pyrite) are available. The main
690 goals of this study were therefore:

- 691 - to better understand denitrification processes in complex systems (water-rock-organic
692 matter-microorganisms) using experiments and numerical modelling of elementary
693 processes and,
- 694 - to conceptualize numerical modelling based on a decoupled thermodynamic database
695 that enables the integration of the new thermo-kinetic approach of Jin and Bethke
696 (2002), clearly splitting available energy in terms of three driving forces, i.e.
697 catabolism, anabolism and a surviving reserve.

698

699 This new, comprehensive thermokinetic rate law based on energetic approaches takes into
700 consideration both the thermodynamic driving force and biogeochemical processes. This
701 approach is applied successfully to the heterotrophic denitrification processes in the presence
702 of acetate coupled with the autotrophic contribution based on pyrite oxidation.

703

704 The thermodynamic and kinetic parameters incorporated in the geochemical code PHREEQC
705 reproduce the concentrations of nitrate-bearing species during the entire duration of the batch
706 experiment. This computer code is robust enough to model the behaviour of chemical species
707 (electron donor, electron acceptor, pH, etc.), biological aspects (anabolism and catabolism of
708 the biomass population) and energy conditions (thermodynamic factor linked to the reaction
709 energy). The comparison of model and observed results confirms that each step of nitrate
710 reduction in the presence of acetate is governed mainly by kinetic factors and not limited by
711 thermodynamic constraints. The energies of the reactions (in the presence of an electron
712 donor like acetate) are too high compared to the energy needed by micro-organisms to
713 proliferate. Consequently, this factor is not limiting and nitrate reduction is complete if there
714 is an excess of electron donors.

715

716 Nevertheless, although this thermodynamic approach is not useful for denitrification with
717 acetate, it cannot be applied to all denitrification processes in the presence of other electron
718 donors. The main factor influencing the thermodynamic factor is the free enthalpy of the
719 reactions – the reactions with acetate and pyrite are very energetic (several hundreds of kJ
720 mol⁻¹) whereas the free standard enthalpy of reactions with goethite or amorphous iron
721 hydroxides are low (several tens of kJ mol⁻¹). This approach should, therefore, be of value for
722 dealing with denitrification involving goethite or amorphous oxides as electron donors.

723

724 This work, which uses both batch and column experiments, shows that these two approaches
725 are complementary. The kinetic data set determined at the batch scale (similar to literature
726 data) is sufficiently well constrained to simulate nitrate, nitrite and biomass concentrations.
727 The numerical simulations indicate that during the heterotrophic denitrification reaction,
728 about 40 % of the carbon from acetate is used for anabolism, whereas 60 % is used for
729 catabolism. Moreover, this set of parameters, fitted with results from batch experiments, can
730 be successfully used to model the column experiment, a 1D system. The heterotrophic
731 denitrification in the column and batch experiments can be explained by the same process,
732 which is promising for application to field studies. Numerical modelling is therefore a useful
733 tool for managing natural environments when the numerous thermo-kinetic parameters are
734 known.

735

736 **ACKNOWLEDGEMENT**

737 We thank C. Crouzet and S. Touzelet (BRGM/Metrology, Monitoring and Analysis Division)
738 for their assistance with experiments and chemical analyses, and S. Kremer (BRGM/Water
739 Division) for her help modifying geochemical databases. The authors also thank two
740 anonymous reviewers for helpful comments and suggestions.

741

742 **REFERENCES**

- 743 Aelion, C.M., Wartinger, U., 2010. Low sulfide concentrations affect nitrate transformations
744 in freshwater and saline coastal retention pond sediments. *Soil Biol. Biochem.*, 41(4),
745 735-741.
- 746 Aminzadeh, B., Torabian, A., Azimi, A.A., Nabi Bidhendi, Gh.R., Mehrdadi, N., 2010. Salt
747 inhibition effects on simultaneous heterotrophic/autotrophic denitrification of high
748 nitrate wastewater. *Int. J. Environ. Res.*, 4(2), 255-262.
- 749 Aslan, S., 2005. Combined removal of pesticides and nitrates in drinking waters using
750 biodenitrification and sand filter system. *Process Biochem.*, 40, 417-424.
- 751 Bishop, P.L., Yu, T., 1999. A microelectrode study of redox potential change in biofilms.
752 *Water Sci. Technol.*, 39(7), 179-185.
- 753 Bowden, W.B., 1987. The biogeochemistry of nitrogen in freshwater wetlands.
754 *Biogeochemistry*, 4, 313-348.

- 755 Chapelle, F.H., 2001. *Ground-Water Microbiology and Geochemistry*, 2nd ed. New York:
756 John Wiley and Sons.
- 757 Clément, T.P., Peyton, B.M., Skeen, R.S., Jennings, D.A., Petersen J.N., 1997. Microbial
758 growth and transport in porous media under denitrification conditions: experiments
759 and simulations. *J. Cont. Hydrol.*, 24, 269-285.
- 760 Cord-Ruwisch, R., Seitz, H., Conrad, R., 1988. The capacity of hydrogenotrophic anaerobic
761 bacteria to compete for traces of hydrogen depends on the redox potential of the
762 terminal electron acceptor. *Arch. Microbiol.*, 149, 350-357.
- 763 Curtis, G.P., 2003. Comparison of approaches for simulating reactive solute transport
764 involving organic degradation reactions by multiple terminal electron acceptors.
765 *Computers and Geosciences*, 29, 319–329.
- 766 Dahab, M.F., 1987. Treatment alternatives for nitrate contaminated groundwater supplies. *J.*
767 *Environ. Syst.* 17, 65-75.
- 768 Decker, K., Jungermann, K., Thauer, R.K., 1970. Energy production in anerobic organism.
769 *Angew. Chem. Int. Ed. Engl.* 9, 138-158.
- 770 Devlin, J.F., Eedy, R., Butler, B.J., 2000. The effects of electron donor and granular iron on
771 nitrate transformation rates in sediments from a municipal water supply aquifer. *J.*
772 *Cont. Hydrol.*, 46, 81-97.
- 773 Dommergues, Y., Mangenot, F., 1970. *Ecologie microbienne du sol*. Masson Ed., Paris, 783
774 pp.
- 775 Duff, J.H., Triska, F.J., 1990. Denitrification in sediments from the hyporheic zone adjacent
776 to a small forested stream. *Can. J. Fish. Aquat. Sci.*, 47, 1140-1147.
- 777 Ehrlich, H.L., 2002. *Geomicrobiology*. 4th edition. New York: Marcel Dekker, 768 pp.
- 778 Fennell, D.E., Gossett, J.M., 1998. Modeling the production of and competition for hydrogen
779 in a dechlorinating culture. *Environ. Sci. Technol.*, 32, 2450-2460.
- 780 Giraldo-Gomez, E., Goodwin, S., Switzenbaum, M. 1992. Influence of mass transfer
781 limitations on determination of the half saturation constant for hydrogen uptake in a
782 mixed-culture CH₄-producing enrichment. *Biotechnol. Bioeng.*, 40, 768-769.
- 783 Gommers, P.J.F., Buleveld W., Zuijderwijk, F.J.M., Kuenen, J.G., 1988. Simultaneous sulfide
784 and acetate oxidation in a denitrifying fluidized bed reactor—II. Measurements of
785 activities and conversion. *Wat. Res.*, 22(9), 1085-1092.
- 786 Greskowiak, J., Prommer, H., Vanderzalm, J., Pavelic, P., Dillon, P., 2005. Modeling of
787 carbon cycling and biogeochemical changes during injection and recovery of
788 reclaimed water at Bolivar, South Australia. *Water Resour. Res.*, 41, W10418.

789 Halvorson, H.O., Ziegler, N.R., 1933. Applications of statistics to problems in bacteriology. I.
790 A means of determining bacterial population by the dilution method. *J. Bacteriol.*, 25,
791 101-121.

792 Her, J.J., Huang, J.S., 1995. Influence of carbon source and C/N ratio on nitrate/nitrite
793 denitrification and carbon breakthrough. *Bioresour. Technol.*, 54, 45–51.

794 Hoh, C.Y., Cord-Ruwisch, R., 1996. A practical kinetic model that considers end product
795 inhibition in anaerobic digestion processes by including the equilibrium constant.
796 *Biotechnol. Bioengin.* 51, 597-604.

797 Hunter, K.S., Wang, Y., Van Cappellen, P., 1998. Kinetic modeling of microbially-driven
798 redox chemistry of subsurface environments: coupling transport, microbial
799 metabolism and geochemistry. *J. Hydrol.*, 209, 53-80.

800 Istok, J.D., Park, M., Michalsen, M., Spain, A.M., Krumholz, L.R., Liu, C., McKinley, J.,
801 Long, P., Roden, E., Peacock, A.D., Baldwin, B., 2010. A thermodynamically-based
802 model for predicting microbial growth and community composition coupled to system
803 geochemistry: Application to uranium bioreduction. *J. Cont. Hydrol.*, 112, 1-14.

804 Jin, Q., Bethke, C.M., 2002. Kinetics of electron transfer through the respiratory chain.
805 *Biophys. J.* 83, 1797-1808.

806 Jin, Q., Bethke, C.M., 2003. A new rate law describing microbial respiration. *Appl. Env.*
807 *Microb.* 69, 2340-2348.

808 Jin, Q., Bethke, C.M., 2005. Predicting the rate of microbial respiration in geochemical
809 environments. *Geochim. Cosmochim. Acta* 69, 1133-1143.

810 Jin, Q., Bethke, C.M., 2007. The thermodynamics and kinetics of microbial metabolism. *Am.*
811 *J. Sc.*, 307, 643-677.

812 Jones, J.B., Fisher, S.G., Grimm, N.B., 1995. Nitrification in the hyporheic zone of a desert
813 stream ecosystem. *J. N. Am. Benthol. Soc.*, 14(2), 249–258.

814 Keating, E.H., Bahr, J.M., 1998. Reactive transport modeling of redox geochemistry:
815 Approaches to chemical disequilibrium and reaction rate estimation at a site in
816 northern Wisconsin. *Water Resour. Res.*, 34, 3573-3584.

817 Kelso, B.H.L., Smith, R.V., Laughlin, R.J., 1999. Effects of carbon substrates on nitrite
818 accumulation in freshwater sediments. *Appl. Environ. Microbiol.*, 65(1), 61-66.

819 Kleerebezem, R., Stams, A.J.M., 2000. Kinetics of syntrophic cultures: a theoretical treatise
820 on butyrate fermentation. *Biotechnol. Bioengin.*, 67, 528-543.

- 821 Knab, N.J., Dale, A.W., Lettmann, K., Fossing, H., Jørgensen, B.B., 2008. Thermodynamic
822 and kinetic control on anaerobic oxidation of methane in marine sediments. *Geochim.*
823 *Cosmochim. Acta*, 72, 3746-3757.
- 824 Knowles, R., 1982. Denitrification. *Microb. Rev.* 46, 43-70.
- 825 Koenig, A., Liu L.H., 2001. Kinetic model of autotrophic denitrification in sulphur packed-
826 bed reactors. *Water Res.*, 35, 1969–1978.
- 827 Lindberg, R.D., Runnels, M.D., 1984. Ground water redox reactions: an analysis of
828 equilibrium state applied to Eh measurements and geochemical modelling. *Science*
829 225, 925-927.
- 830 Lasaga, A.C., 1984. Chemical kinetics of water-rock interactions. *J. Geophys. Res.*, 89, 4009–
831 4025.
- 832 Lovley, D.R. 1985. Minimum threshold for hydrogen metabolism in methanogenic bacteria.
833 *Appl. Environ. Microbiol.*, 49, 1530-1531.
- 834 Lovley, D.R., Chapelle, F.H., 1995. Deep subsurface microbial processes. *Rev. Geophys.*, 3,
835 365–381
- 836 McCallum, J.E., Ryan, M.C., Mayer, B., Rodvang, S.J., 2008. Mixing-induced groundwater
837 denitrification beneath a manured field in southern Alberta, Canada. *Appl. Geochem.*,
838 23(8), 2146-2155.
- 839 Madigan, M.T., Martinko J.M., Parker, J., 2000. *Brock Biology of Microorganisms*. 9th
840 edition. Prentice Hall, Upper Saddle River, NJ.
- 841 Marchand, E.A., Silverstein, J., 2002. Influence of heterotrophic microbial growth on
842 biological oxidation of pyrite. *Environ. Sci. Technol.*, 36, 5483-5490.
- 843 Matějů, V., Čížinská, S., Krejčí, J., Janoch, T., 1992. Biological water denitrification - A
844 review. *Enzyme Microb. Technol.*, 14, 170-183.
- 845 Michaelis, L., Menten, M.L., 1913. Die Kinetik der Invertinwirkung. *Biochemische*
846 *Zeitschrift*, 49, 333–369.
- 847 Michard, G., 2002. *Chimie des eaux naturelles. Principe de Géochimie des Eaux*. Editions
848 PUBLISUD, 461 p.
- 849 Mitchell, P., 1961. Coupling of phosphorylation to electron and hydrogen transfer by a
850 chemiosmotic type of mechanism. *Nature*, 191, 144-148.
- 851 Molénat, J., Durand, P., Gascuel-Oudou, C., Davy, P., Gruau, G., 2002. Mechanisms of
852 nitrate transfer from soil to stream in an agricultural watershed of French Brittany.
853 *Wat. Air Soil Pollut.*, 133, 161–183.
- 854 Monod, J., 1949. The growth of bacterial cultures. *Ann. Rev. Microbiol.* 3, 371-393.

855 Noguera, D.R., Brusseau, G.A., Rittmann, B.E., Stahl., D.A., 1998. Unified model describing
856 the role of hydrogen in the growth of *Desulfovibrio Vulgaris* under different
857 environmental conditions. *Biotechnol. Bioengin.* 59, 732-746.

858 Odencrantz, J.E., Bae, W., Valocchi, A.J., Rittmann, B.E., 1990. Stimulation of biologically
859 active zones (BAZ's) in porous media by electron-acceptor injection. *J. Cont. Hydrol.*,
860 6, 37-52.

861 Oh, S.E., Bum, M.S., Yoo, Y.B., Zubair, A., Kim, I.S., 2002. Nitrate removal by simultaneous
862 sulfur utilizing autotrophic and heterotrophic denitrification under different organics
863 and alkalinity conditions: batch experiments. *Wat. Sci. Technol.*, 47(1), 237-244.

864 Palandri, J.L., Kharaka, Y.K, 2004. A compilation of rate parameters of water-mineral
865 interaction kinetics for application to geochemical modeling: U.S. Geological Survey
866 Water-Resources Investigations Report 04-1068.

867 Park, J.Y., Yoo, Y.J., 2009. Biological nitrate removal in industrial wastewater treatment:
868 which electron donor we can choose. *Appl. Microbiol. Biotechnol.*, 82, 415–429.

869 Parkhurst, D.L., Appelo C.A.J., 1999. User's guide to PHREEQC (version 2): A computer
870 program for speciation, batch-reaction, one-dimensional transport, and inverse
871 geochemical calculations. U.S. Geological Survey Water-Resources Investigations
872 Report 99-4259, 312 p.

873 Pauwels, H., Kloppmann, W., Foucher, J-C., Martelat, A., Fritsche, V., 1998. Field tracer test
874 for denitrification in a pyrite-bearing schist aquifer. *Appl. Geochem.* 13(6), 767-778.

875 Pauwels, H., Lachassagne, P., Bordenave, P., Foucher, J.-C., Martelat, A., 2001. Temporal
876 variability of nitrate concentration in a schist aquifer and transfer to surface waters.
877 *Appl. Geochem.* 16(6), 583-596.

878 Pauwels, H, Talbo, H., 2004 - Nitrates concentration in wetlands: assessing the contribution
879 of different water bodies from anion concentrations. *Water Research*, 38, 1019-1025.

880 Pauwels, H., Ayraud, V., Aquilina, L., Molénat, J., 2010. The fate of nitrogen and sulfur in
881 hard-rock aquifers as shown by sulfate-isotope tracing. *Appl. Geochem.* 25(1), 105-
882 115.

883 Peyton, B.M., Mormile, M.R., Petersen, J.N., 2001. Nitrate reduction with *Halomonas*
884 *Campisalis*: kinetics of denitrification at pH 9 and 12.5% NaCl. *Water Res.*, 35, 4237-
885 4242.

886 Pinay, G., Burt, T.P., 2001. Nitrogen Control by Landscape Structures. Research Project
887 1997-2000, EC DGXII. Environment and Climate: ENV4-CT97-0395, February 2001.
888 Final Report 1997–2000.

889 Postma, D., Boesen, C., Kristiansen, H., Larsen F., 1991. Nitrate reduction in an unconfined
890 sandy aquifer: water chemistry, reduction processes and geochemical modeling. *Water*
891 *Resour. Res.* 27, 2027-2045.

892 Rittmann, B.E., McCarty, P.L., 2001. *Environmental Biotechnology: Principles and*
893 *Applications*. McGraw-Hill Companies, Inc., New York (USA), 754 pp.

894 Rivett, M.O., Buss, S.R., Morgan, P., Smith, J.W.N., Bemment, C.D., 2008. Nitrate
895 attenuation in groundwater: A review of biogeochemical controlling processes. *Water*
896 *Res.*, 42, 4215-4232.

897 Ruiz, L., Abiven, S., Durand, P., Martin, C., Vertes, F., Beaujouan, V., 2002. Effect on nitrate
898 concentration in stream water of agricultural practices in small catchments in Brittany:
899 I. Annual nitrogen budgets. *Hydrol. Earth Syst. Sci.* 6, 507–513.

900 Schipper, L., Vojvodic Vukovic, M., 1998. Nitrate Removal from Groundwater using a
901 Denitrification Wall Amended with Sawdust: Field Trial. *J. Environ. Qual.* 27, 664-
902 668.

903 Schipper, L., Vojvodic Vukovic, M., 2000. Nitrate Removal from Groundwater and
904 Denitrification Rates in a Porous Treatment wall Amended with Sawdust. *Ecol. Eng.*
905 14, 269-278.

906 Scott J.T., McCarthy, M.J., Gardner, W.S., Doyle, R.D., 2008. Denitrification, dissimilatory
907 nitrate reduction to ammonium, and nitrogen fixation along a nitrate concentration
908 gradient in a created freshwater wetland. *Biogeochemistry*, 87, 99–111.

909 Sheibley, R.W., Jackman, A.P., Duff, J.H., Triska, F.J., 2003. Numerical modeling of coupled
910 nitrification–denitrification in sediment perfusion cores from the hyporheic zone of the
911 Shingobee River, MN. *Adv. Water Resour.*, 26(9), 977-987.

912 Sigg, L., Behra, P., Stumm, W., 2000. *Chimie des milieux aquatiques; chimie des eaux naturelles et des*
913 *interfaces dans l'environnement*, 3rd ed. Paris: Dunod.

914 Squillace, P.J., Scott, J.C., Moran, M.J., Nolan, B.T., Kolpin, D.W., 2002. VOCs, pesticides,
915 nitrate, and their mixtures in ground-water used for drinking water in the United
916 States. *Environ. Sci. Technol.*, 36, 1923–1930.

917 Starr, R.C., Gillham R.W., 1993. Denitrification and organic carbon availability in two
918 aquifers. *Ground Water*, 31, 934-947.

919 Stefansson, A., Arnorsson, S. and Sveinbjörnsdottir, A.E., 2005. Redox reactions and
920 potentials in natural waters at disequilibrium. *Chem. Geol.*, 221, 289-311.

921 Stevenson, F.J., Cole, M.A., 1999. *Cycles of soil: carbon, nitrogen, phosphorus, sulfur,*
922 *micronutrients*. 2nd Edition, John Wiley and Sons, 427 pages.

923 Tarits, C., Aquilina, L., Ayraud, V., Pauwels, H., Davy, P., Touchard, F. and Bour, O., 2006.
924 Oxido-reduction sequence related to flux variations of groundwater from a fractured
925 basement aquifer (Ploemeur area, France). *Appl. Geochem.*, 21(1), 29-47.

926 Tavares, P., Pereira, A.S., Moura, J.J.G., Moura, I., 2006. Metalloenzymes of the
927 denitrification pathway. *J. Inorganic Biochem.*, 100, 2087-2100.

928 Torres, C.I., Marcus, A.K., Lee, H.-S., Parameswaran, P., Krajmalnik-Brown, R., Rittmann,
929 B.E., 2010. A kinetic perspective on extracellular electron transfer by anode-respiring
930 bacteria. *FEMS Microbiol. Rev.*, 34, 3–17.

931 Tranvik, L.J., Höfle, M.G., 1987. Bacterial Growth in Mixed Cultures on Dissolved Organic
932 Carbon from Humic and Clear Waters. *Appl. Environ. Microbiol.*, 53(3): 482-488.

933 Tsai, Y.P., Wu, W.M., 2005. Estimating biomass of heterotrophic and autotrophic bacteria by
934 our batch tests. *Environ. Technol.*, 26(6), 601-614.

935 Van Beer, C.G.E.M., 2000. Redox processes active in denitrification. Chapter 12 in: *Redox:
936 fundamentals, processes and applications*. Springer-Verlag Berlin Heidelberg New-
937 York, Inc, 110 Figures, 21 Tables.

938 Van Rijn, J., Tal, Y., 1996. Influence of volatile fatty acids on nitrite accumulation by a
939 *Pseudomonas stutzeri* strain isolated from a denitrifying fluidized bed reactor. *Appl.
940 Environ. Microbiol.*, 62(7), 2615-2620.

941 Weber, K.A., Picardal, F.W., Roden, E.E., 2001. Microbially catalysed nitrate-dependent
942 oxidation of biogenic solid-phase Fe(II) compounds. *Environ. Sci. Technol.*, 35, 1644-
943 1650.

944 Wilderer, P.A., Jones, W.L., Dau, U., 1987. Competition in denitrification systems affecting
945 reduction rate and accumulation of nitrite. *Water Res.*, 21(2), 239-245.

946 White, D., 1995. *The physiology and biochemistry of prokaryotes*. Oxford University Press,
947 New York, N.Y.

948 Whitmire, S.L., Hamilton, S.K., 2005. Rapid removal of nitrate and sulfate in freshwater
949 wetland sediments. *J. Environ. Qual.*, 34, 2062–2071.

950 Yu, T., Bishop, P.L., 1998. Stratification of microbial metabolic processes and redox potential
951 change in an aerobic biofilm studied using microelectrodes. *Water Sci. Technol.*,
952 37(4), 195–198.

953
954

Figure Captions

- 955
- 956
- 957 Fig. 1. Schematic representation of the flow-through column
- 958 Fig. 2. Evolution with time of the concentration of N-bearing species. Symbols correspond to
959 experimental data with error bars. Lines represent modelling results
- 960 Fig. 3. Evolution with time of pH. Points and dashed lines correspond to measured data of the
961 three replicates. The solid line represents calculated pH values
- 962 Fig. 4. Evolution with time of acetate concentration. Points with dotted lines correspond to
963 measured data of the three replicates. The bold lines represent calculated values: dashed
964 bold line = calculation without considering the bacterial anabolism; solid bold line =
965 calculation with anabolism and catabolism
- 966 Fig. 5. Evolution with time of biomass concentration. Points and dotted lines correspond to
967 measured data for the three replicates. The solid line represents calculated values.
- 968 Fig. 6. Variations of kinetic factors (F_D , F_A) and the thermodynamic factor (F_T) for nitrate
969 reduction (Eq. 2) versus nitrate concentration
- 970 Fig. 7. Variations of kinetic factors (F_D , F_A) and the thermodynamic factor (F_T) for nitrite
971 reduction (Eq. 3) versus time
- 972 Fig. 8. Nitrate and nitrite concentrations at the outlet of the column. Symbols represent
973 experimental data and lines correspond to numerical simulation results.
- 974 Fig. 9. Evolution of sulphate and chloride concentrations. Symbols represent Cl^- and SO_4^{2-}
975 concentrations in the aqueous solution at the outlet. Dashed and dotted lines correspond
976 to Cl^- and SO_4^{2-} concentrations in the solution at the inlet. The solid line represents
977 calculated sulphate concentration at the outlet of the column.
- 978
- 979

980
981
982
983
984
985
986
987
988
989
990
991
992
993
994
995
996

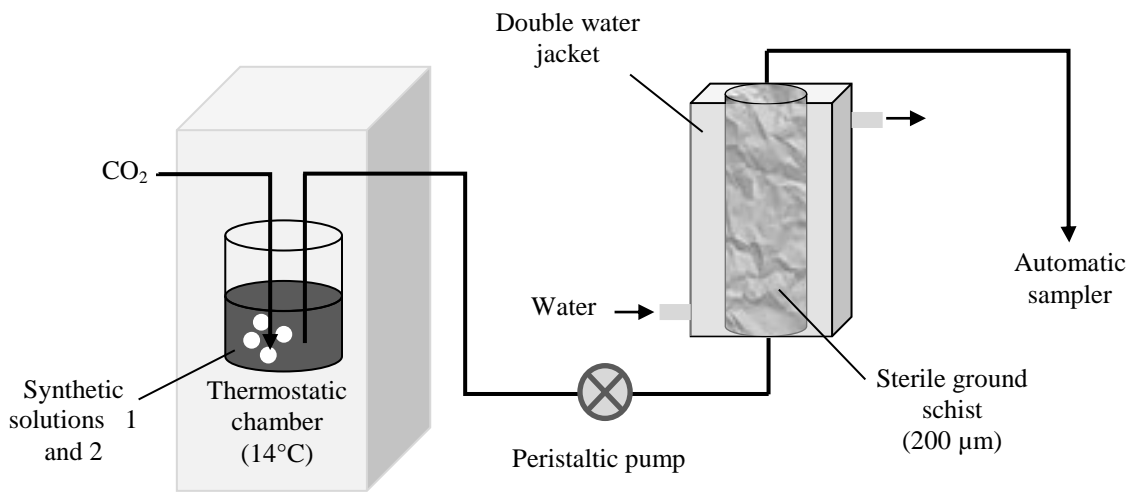


Fig. 1

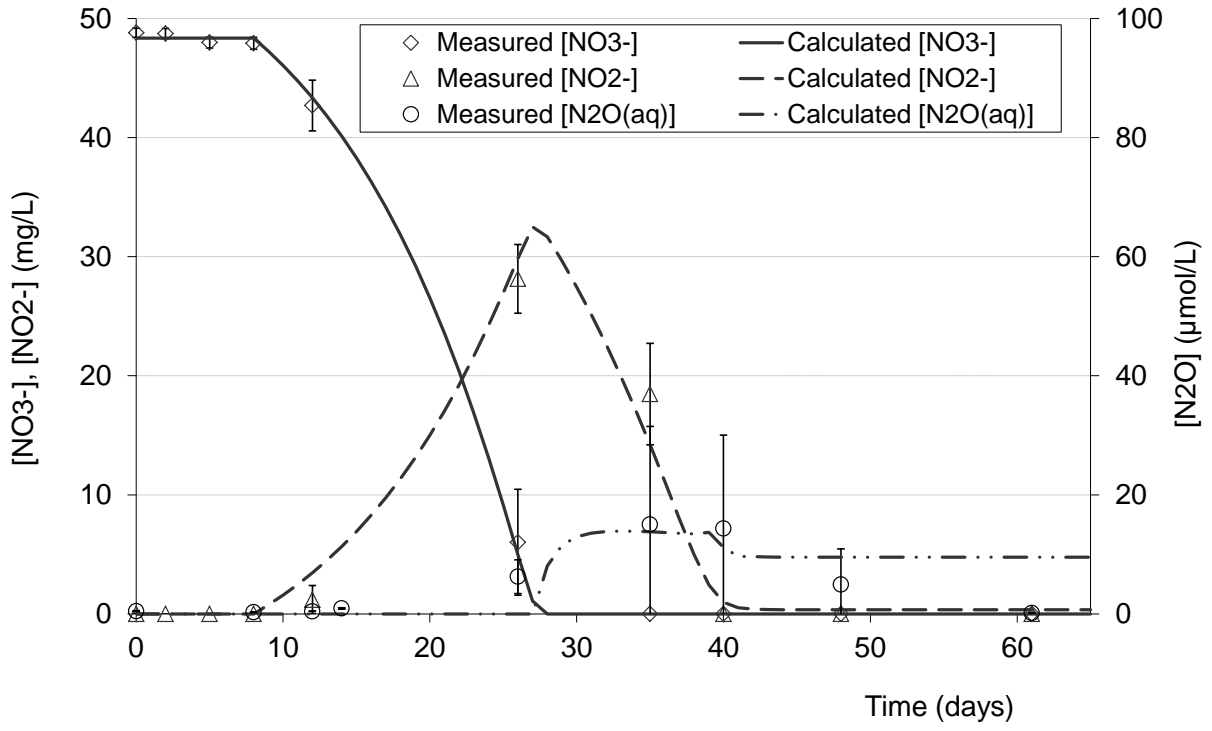


Fig. 2

997
998
999

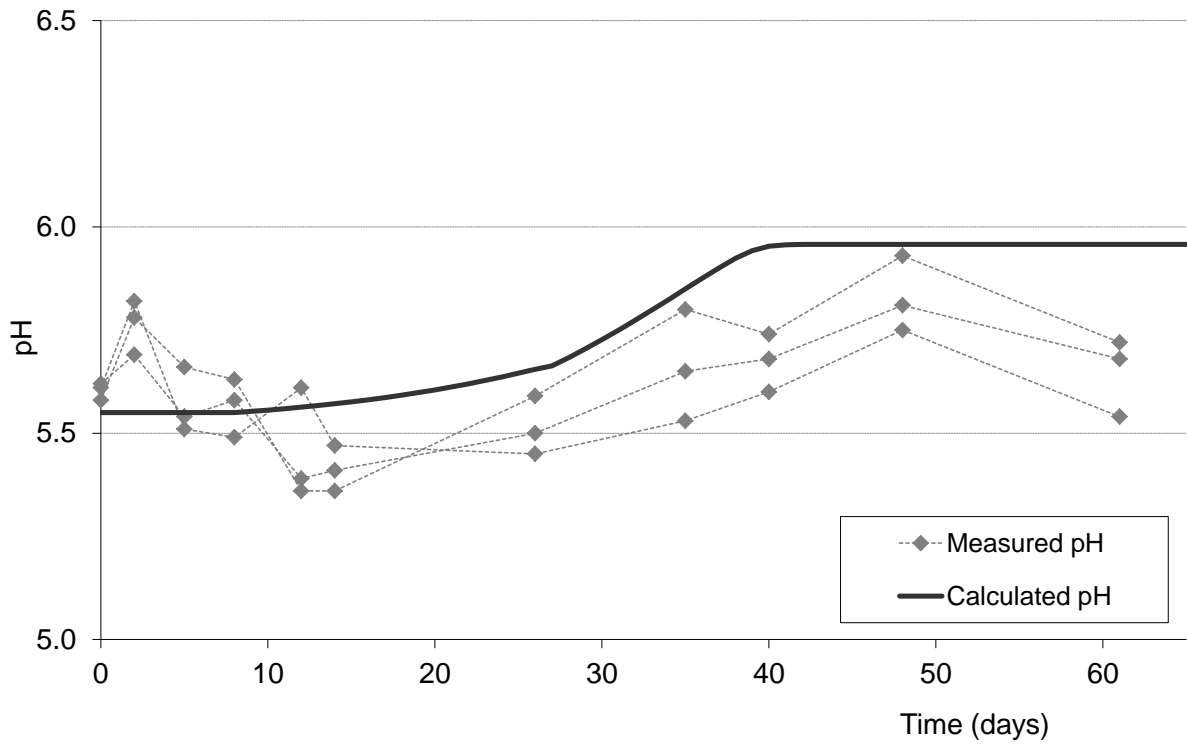


Fig. 3

1000
1001
1002
1003

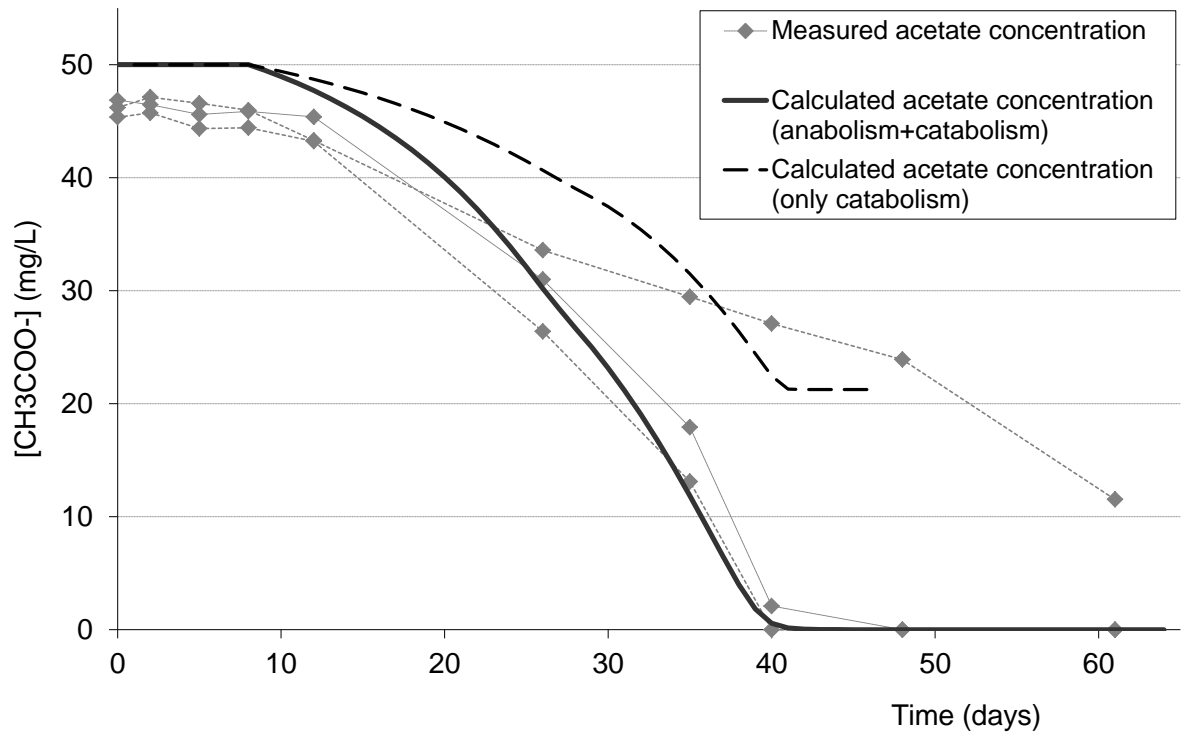


Fig. 4

1004
1005
1006
1007
1008

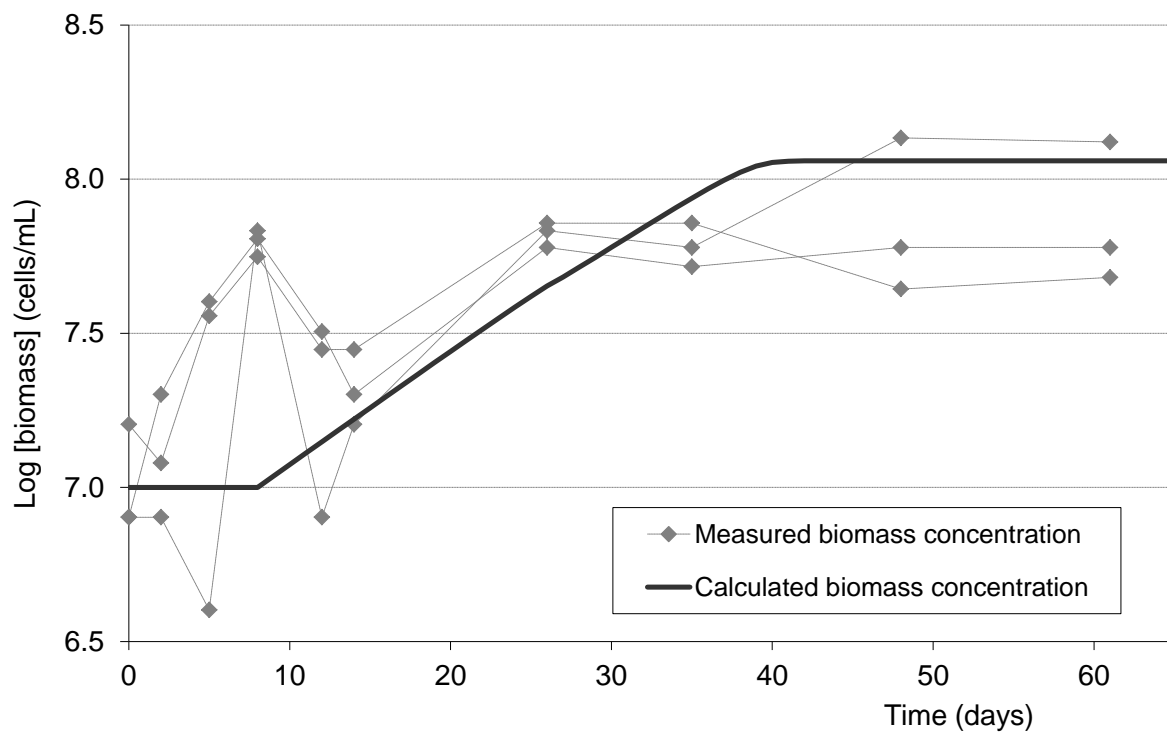


Fig. 5

1009
1010
1011
1012

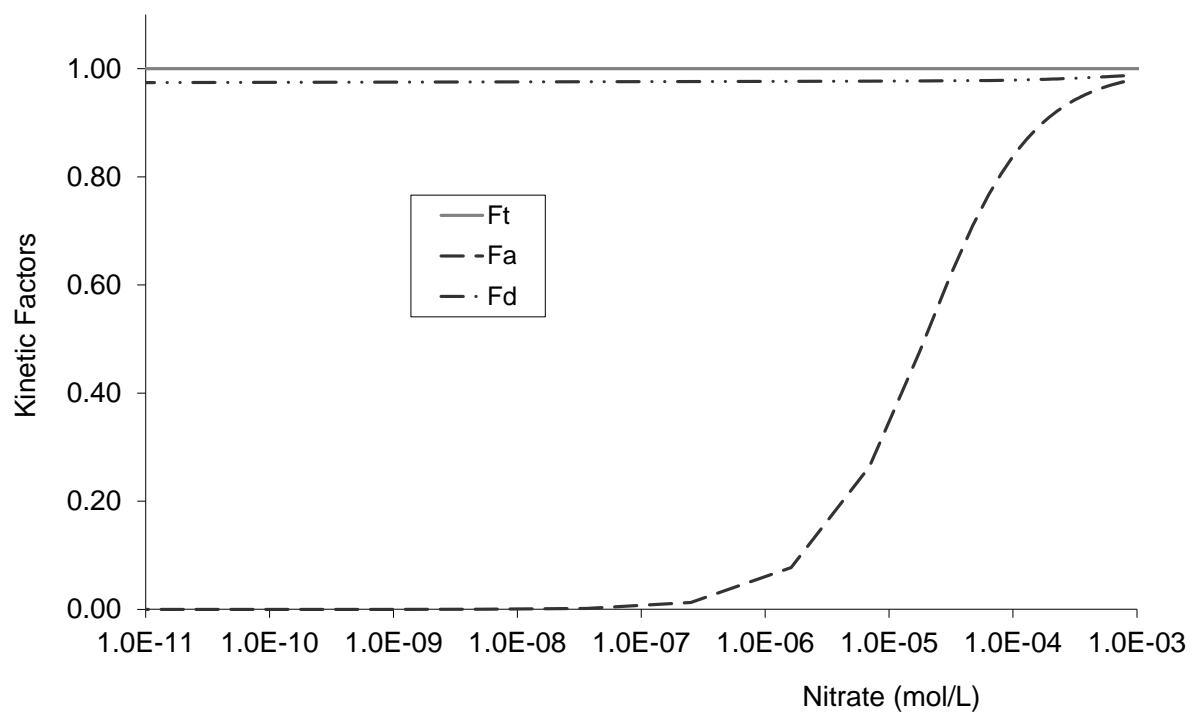


Fig. 6

1013
1014
1015
1016

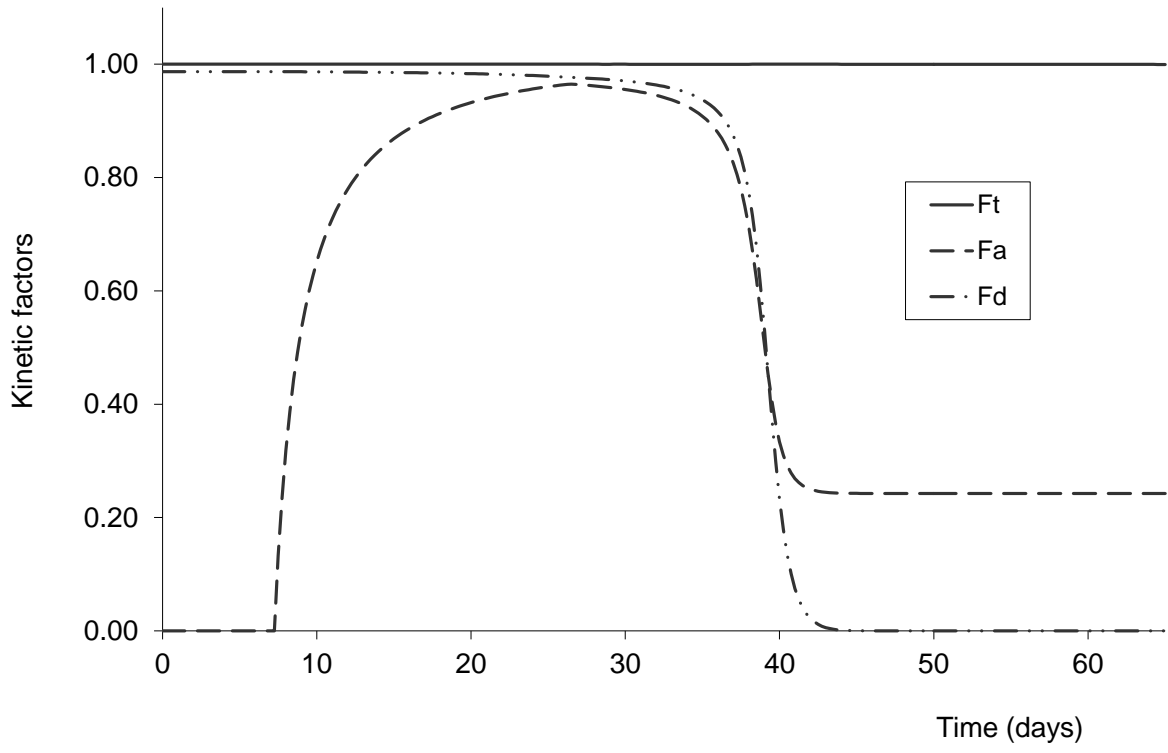


Fig. 7

1017
1018
1019
1020
1021

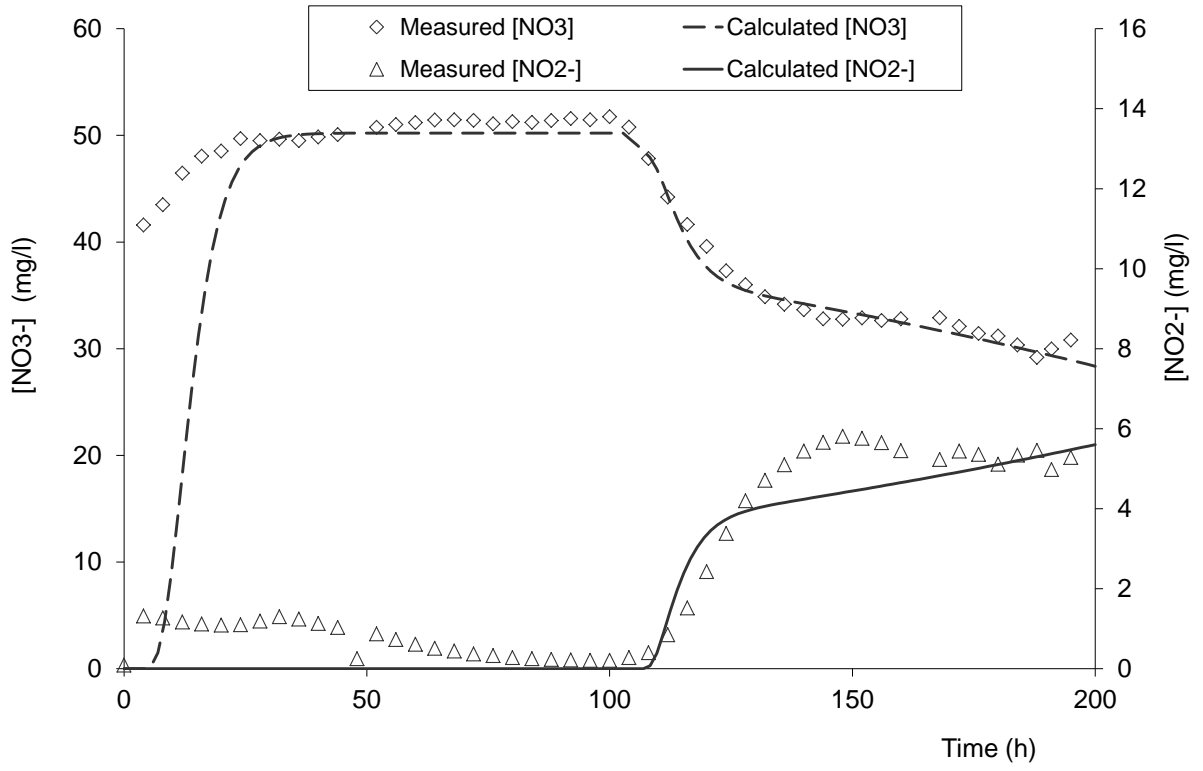


Fig. 8

1022
 1023
 1024
 1025

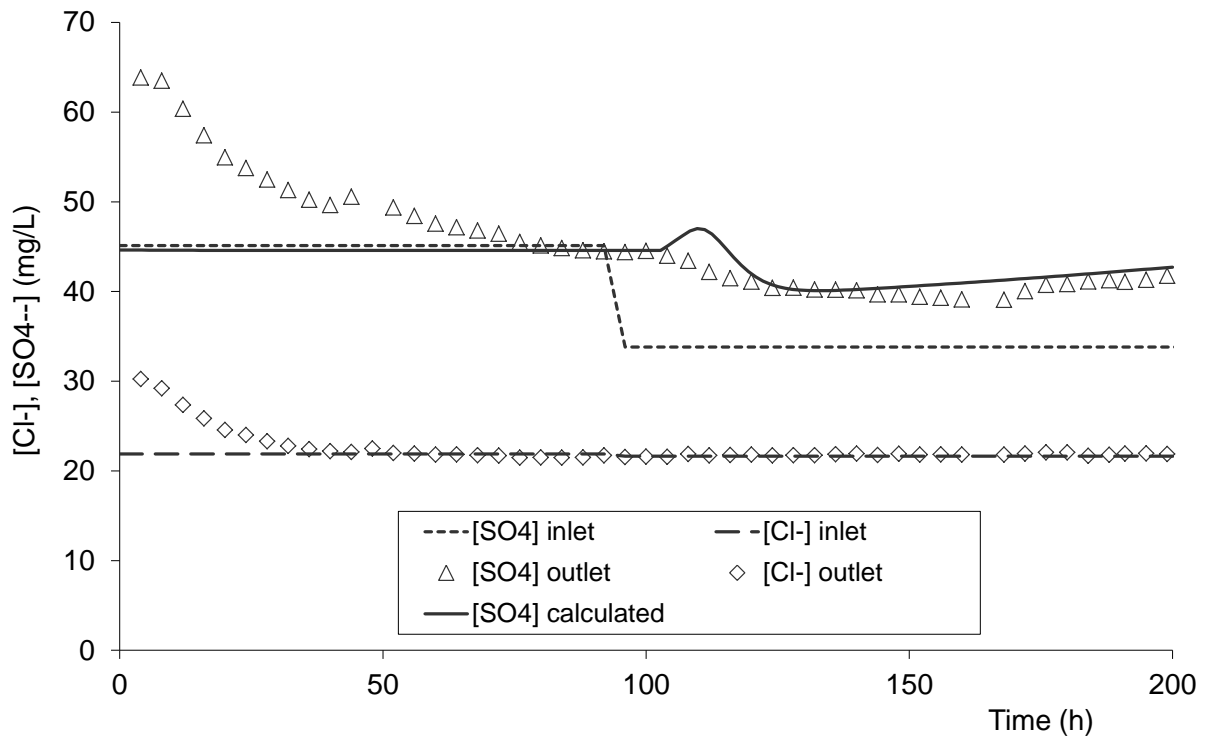


Fig. 9

1026
1027
1028

1029

Table 1: Chemical composition of the groundwater (in mmol kg⁻¹_{H2O})

Chemicals	pH	Eh (mV)	Alk	Ca	Mg	Na	K	Cl	NO ₃	SO ₄	Fe	DOC
Concentration	6.68	179	0.77	0.38	0.36	0.80	0.03	0.78	<LOQ	0.33	0.13	0.058

1030

1031

1032

LOQ = Limit of Quantification

1033

Table 2: Mineralogical composition of the aquifer formation

Minerals	Composition (in wt%)
Quartz	20-25
Chlorite	40-45
Mica / Illite	30-35
Pyrite	0.1
Plagioclases	5
Orthose	1
Smectite	0.5

1034

1035

1036

1037

Table 3 Chemical compositions and concentrations of the synthetic solutions

Chemical species	Concentration (mg L ⁻¹)	
	Synthetic solution 1	Synthetic solution 2
Ca ²⁺	11.60	11.60
Mg ²⁺	11.40	8.60
K ⁺	1.10	1.10
Na ⁺	30.40	40.00
Cl ⁻	21.60	21.60
HCO ₃ ⁻	30.50	30.50
SO ₄ ²⁻	45.10	33.80
NO ₃ ⁻	50.00	50.00
CH ₃ COO ⁻	/	24.80

1038

1039

1040

1041

1042

1043